

Non-invasive multimodal functional imaging of the intestine with frozen micellar naphthalocyanines

Yumiao Zhang, Mansik Jeon, Laurie J. Rich, Hao Hong, Jumin Geng, Yin Zhang, Sixiang Shi, Todd E. Barnhart, Paschalis Alexandridis, Jan D. Huizinga, Mukund Seshadri, Weibo Cai, Chulhong Kim and Jonathan F. Lovell

Supplementary Information Contents:

- **Methods**
- **Supplementary Figure 1:** Yield of nanonaps as a function of initial F127 concentration
- **Supplementary Figure 2:** Calibration curve used to determine free F127 concentration during centrifugal washing
- **Supplementary Figure 3:** Contact angle analysis of washing cycles
- **Supplementary Table 1:** Nanonap optical parameters
- **Supplementary Figure 4:** Normalized absorbance spectrum of Nc dyes in dichloromethane and in aqueous nanonaps
- **Supplementary Figure 5:** Self-quenched fluorescence emission of ZnBNc nanonaps.
- **Supplementary Figure 6:** X-ray diffraction spectrum of ZnBNc nanonaps and pure ZnBNc
- **Supplementary Figure 7:** Photoacoustic spectra of ZnBNc, BNc and ONc nanonaps
- **Supplementary Figure 8:** Nanonaps maintain near neutral zeta potential over broad pH range
- **Supplementary Figure 9:** Resonance scattering spectra of nanonaps and gold nanorods
- **Supplementary Figure 10:** Nanonaps, but not gold nanorods, are stable in simulated gastric and intestinal fluid
- **Supplementary Figure 11:** Photoacoustic spectra of concentration matched nanonaps and gold nanorods
- **Supplementary Figure 12:** Caco-2 cell viability following incubation with nanonaps or methylene blue.
- **Supplementary Figure 13:** 50,000 OD₈₆₀/kg nanonaps is a safe orally administered nanonap dose.
- **Supplementary Figure 14:** Lack of motility of nanonaps with 3% v/v isoflurane anesthetization
- **Supplementary Figure 15:** Signal to noise ratio of ZnBNc and ONc nanonaps in a chicken breast phantom
- **Supplementary Table 2:** Labelling of nanonaps with ⁶⁴Cu
- **Supplementary Figure 16:** Copper labelling does not affect nanonap zeta potential or size
- **Supplementary Figure 17:** Faecal clearance of ⁶⁴Cu chelated in nanonaps
- **Supplementary Movie 1 (online):** Real-time, high resolution, multimodal US/PA functional imaging of the intestine
- **Supplementary Movie 2 (online):** Whole body intestinal imaging using PET

Methods:

Materials were obtained from Sigma unless noted otherwise.

Solubilization and retention of dyes with varying hydrophobicity

LogP values were evaluated using the ALOGPS 2.1 program hosted at vcclab.org. 2 mg of methylene blue, quinaldine red, rhodamine 6G, IR780, 2,11,20,29-Tetra-tert-butyl-2,3-naphthalocyanine (BNc), Zinc- 2,11,20,29-Tetra-tert-butyl-2,3-naphthalocyanine (ZnBNc), 5,9,14,18,23,27,32,36-Octabutoxy-2,3-naphthalocyanine (ONc), Nickel-5,9,14,18,23,27,32,36-Octabutoxy-2,3-naphthalocyanine (NiONc), Vanadyl 2,11,20,29-tetra-tert-butyl-2,3-naphthalocyanine (VBNc), 2,9,16,23-Tetra-tert-butyl-29H,31H-phthalocyanine (BPc), Vanadyl 3,10,17,24-tetra-tert-butyl-1,8,15,22-tetrakis(dimethylamino)-29H,31H-phthalocyanine (VBPc) were dissolved in 1 mL dichloromethane or methanol for MB then added dropwise to a 10% w/v solution of Pluronic F127 (Sigma #P2443). The solution was stirred in a fume hood at room temperature (or 80 °C for MB) for 4 hours to evaporate the organic solvent. After centrifugation at 4000xg for 5 minutes to remove any large aggregates, 100 µL of supernatant was diluted in 3 mL of 20 mM sodium cholate solution. After recording the absorbance, the solution was placed in dialysis tubing (Fisher, #21-152-16; nominal molecular weight cut-off of 12,000 -14,000 Daltons) and dialyzed against 500 mL of 20 mM sodium cholate buffer at room temperature. The buffer was changed after

4 hours. After 24 hours, the absorbance of the solution in dialysis tubing was measured again to determine dye retention percentage.

Nanonap formation

Nanonaps were synthesized by a modified nanoprecipitation method. Briefly, 2 mg Nc or Pc dye was dissolved in 1 mL dichloromethane was added dropwise to an aqueous solution of 10 mL F127 (10%, w/v). Dichloromethane was chosen since the dyes were all found to be soluble (>10 mg/mL), whereas methanol solubility was less than 0.1 mg/mL. The suspension was stirred in a fume hood at room temperature for 4 hours to evaporate the dichloromethane. After centrifugation at 4000xg for 5 minutes to remove aggregates, the supernatant was used for CMC switching purification. To remove unincorporated F127, the supernatant was cooled on ice then centrifuged in an Amicon Ultra-15 centrifugal filtration device with a 100,000 MWCO (Fisher #UFC9-100-24) at 4 °C until 200 μ L of solution was retained in the filtration device. The filtrate was stored for determination of F127 and dye concentration. Water was added back to the filtration device and the washing procedure was repeated at least three times.

To quantify incorporated F127, the collected filtrates were collected and F127 concentration was determined by a previously reported colourimetric assay method with minor modifications. In brief, a cobalt thiocyanate reagent was prepared first by dissolving 0.3 g cobalt nitrate hexahydrate and 1.2 g ammonium thiocyanate in 3 mL water. Then 100 μ L cobalt thiocyanate solution, 40 μ L F127 solution in the concentration range of 0-7.5 wt% (more concentrated F127 solutions were diluted to fit the range), 200 μ L ethyl acetate and 80 μ L ethanol were combined. The mixture was vortexed gently and centrifuged at 14000xg for 1 min. The blue supernatant was removed and the blue pellet was washed using ethyl ether several (~5) times until the supernatant became colourless. The pellet was then dissolved in 1 mL acetone to measure the absorbance at 623 nm (Supplementary Fig. 2 shows the standard curve of the cobalt thiocyanate-F127 complex and the concentration of F127). The F127 retention percentage after each wash was calculated by weighing the mass and determination of the mass percentage by the colourimetric assay. The concentrations of dyes were by determined by measuring absorbance.

For reconstitution studies, nanonaps were prepared by the same procedure using 2 mg ONc dye. DMPC liposome were made by dissolving 2 mg of ONc and 19.9 mg of DMPC (corresponding to 95 molar % DMPC) in a small volume of chloroform. After evaporation of the solvent by nitrogen purging, the film was put under vacuum for 1 hour and then rehydrated with 1.5 mL distilled water and sonicated for 30 min. ONc nanonaps and liposomes were then freeze dried overnight (Labconco Freezone). The powder was then resuspended in a minimal volume of water (50 μ L) and the absorbance was recorded. The samples were briefly centrifuged to remove large insoluble aggregates that interfered with absorption baseline.

Characterization of Nanonap Physical and Optical Properties

Size and zeta potential measurement were carried out using dynamic light scattering with a Nano ZS90 Zetasizer (Malvern Instruments). Transmission electron microscopy was performed using a JEM-2010 electron microscope to determine the morphology of an aqueous dispersion of nanonaps negatively stained with 1 % uranyl acetate. Absorbance was measured by with a Lambda 35 UV/VIS spectrophotometer (Perkin Elmer) at room temperature using cuvettes with 1 cm path lengths, except for the high-concentrated spectral shifting analysis which used 10 μ m path-length cuvettes.

X-ray diffraction powder pattern was carried with freeze dried samples on a Rigaku Ultima IV with operating conditions of 40 KV, 44 mA, and 1.76 kW. The source of the diffractometer used was a Cu K α radiation at a 1.54 Å wavelength with a monochromator filter and analysed in a $\Theta/2\Theta$ mode at room temperature. The 2Θ scan data were collected at a 0.030 interval and the scan speed was 0.5 deg/minute. The technique used for measuring intensities was the focusing beam method.

Scattering and fluorescence properties were assessed using a fluorometer (Photon Technology International). To examine the scattering properties of nanonaps (ZnBNC nanonaps with peak absorption at 707 nm) and gold nanorods with 700 nm peak absorption (NanoPartz # A12-10-700) were used and extinction was normalized to 0.05 at 700 nm in water. Resonance scattering was recorded on a fluorometer with slit widths of 2 nm with simultaneous excitation and emission scanning between 600 and 800 nm. Buffer scattering background blanks were recorded and subtracted from the nanoparticle measurements. Normalized fluorescence measurements were made by measuring the emission spectra with 300 nm excitation of absorbance-matched dilute ZnBNC either in nanonap form or directly dissolved in dichloromethane with 4 nm excitation and emission slit widths.

To determine optical parameters, concentrated nanonaps with known absorbance were lyophilized. The mass of nanonap powder was determined and then a portion of the powder was dissolved in dichloromethane to determine concentration and mass of dye. The mass of F127 was then determined based on the difference in total lyophilized mass. To calculate nanoparticle optical properties, the density of the dyes was assumed to be 1 g/cm^3 , since the hydrophobic dyes can be floated/suspended in water and the density of F127 was taken as 1.05 g/cm^3 . The diameter of nanonaps, which are uniformly spherical were measured using dynamic light scattering and were found to be 17 nm, 20 nm, 26 nm, and 20 nm for BPc, ZnBNc, BNc and ONc respectively. The nanonap volume was assumed to exclude water from its interior. Based on the average density and volume of nanonaps, a per particle mass and subsequent number of dyes per particle could be estimated. The optical absorption cross section was calculated as previously described (Dlott *et al.*, J. Opt. Soc. Am. B. 6-977, 1989), assuming a negligible scattering contribution as demonstrated in Supplementary Figure 9.

To assess the stability of nanonaps in simulated gastric fluid (SGF) and simulated intestine fluid (SIF), nanonaps were dialyzed against 200 mL SGF (Ricca, #7108-32) with added pepsin and pancreatin-containing SIF (Ricca #7109-32). Concentrated nanonaps were diluted with SGF and SIF so that the absorbance was close to 1, then dialyzed at 37°C . 860 nm CTAB stabilized gold nanorods and 850nm thiol-PEG-stabilized gold nanorods (NanoRods LLC, #C122-CTAB and C120-PEG) were subjected to dialysis in the same manner.

Nanonap clearance study

Animal experiments were performed in accordance with the University at Buffalo Institutional Animal Care and Use Committee. 6-8 weeks female BALB/c mice (Harlan labs) were starved overnight with free access to water. Food was introduced after gavage. After gavage of 100 ODs ONc nanonaps (3.42 mg) or methylene blue, the mice were transferred to metabolic cages and faeces and urine were collected separately. Faeces and urine were collected at 0, 2, 4, 8, and 24 hours, weighed and kept at 4°C prior to analysis. For determination of recovery percentages, the absorbance of urine and serum samples was measured directly. Tissues or faeces (~50 mg) were dissolved in 2 mL chloroform (methanol for the recovery of methylene blue), and subjected to disruption using a Tissue Tearor homogenizer (Model 985-370) for 30 seconds or until the dyes were dissolved completely. The solutions were centrifuged at $3000 \times g$ for 3 minutes to remove debris and the absorbance of the chloroform containing dyes was measured to determine the recovery. To calibrate the absorbance difference of dyes in nanonaps form and in chloroform, nanonaps were freeze dried overnight and dissolved in same volume of chloroform and absorbances were measured.

Nanonap toxicity

For in vitro studies, 2×10^4 Caco-2 cells (ATCC) were seeded in a 96 well plate in 20% fetal bovine serum in Dulbecco's Modified Eagle Medium. The next day, cells were treated with ONc nanonaps or methylene blue at the indicated concentrations. 24 hours later, media was removed and XTT was added to determine viability measuring absorbance at 450 nm. For in vivo studies, mice (Harlan Labs, 6 week BALB/c mice) were administered 1000 OD₈₆₀ per 20 g of ONc nanonaps by gavage (given in 3 administrations within a 24 hour period) or kept as controls (n=5 per each group of male gavage, female gavage, male control and female control group). Behaviour was monitored every other day and mass was measured weekly. After 2 weeks, mice were sacrificed and organs were harvested. PBS was used to rinse blood and debris. The organs were immersed in 10% neutral buffered formalin (VWR #16004-114) and fixed over 24 hours. The fixed organs were processed through increasing grades of alcohol, cleared in xylene and infiltrated with paraffin (TBS). They were subsequently embedded, cut and stained with haematoxylin and eosin. Finally, the slides were scanned with single slide scanner (Aperio)

Photoacoustic experiments

A custom-built volumetric reflection-mode PAT system using a single element ultrasound transducer was used. In briefly, tunable laser pulses were synthesized from an OPO laser (Surelite OPO PLUS; Continuum; wavelength tuning range, 680 to 2500 nm; pulse width, 5 ns; and pulse repetition rate, 10Hz) excited by a pump laser (SLII-10; Continuum; Q-switched Nd:YAG; 532 nm). An optical wavelength of either 710 or 860 nm, which matched the respective absorption peak of ZnBNc or ONc nanonaps, was used for PA imaging experiments. Generated light passed through a home-made spherical conical lens and optical condenser with a pulse energy of $\sim 5 \text{ mJ/cm}^2$, much less than the safety limit. During the raster scanning for volumetric imaging, the acoustic coupling was improved with a custom-made water tray. The mouse (6-8 weeks female BALB/c mouse) was located below the water tray. The induced PA signals were captured by the focused ultrasound transducer (V308; Olympus NDT; 5-MHz center frequency). A Vevo LAZR US/PA imaging system was used for real-time imaging

with 21 MHz transducer frequency. The movement of nanonaps in the digestive system was photoacoustically monitored after gavage of 100 ODs of nanonaps in female BALB/c mice. This corresponds to 3.4 mg of ONc nanonaps and 13.2 mg of ZnBNc nanonaps. Region of interest analysis was performed with the system software. Rate of peristaltic calculations per minute was determined by taking the 1st derivative of the region of interest intensity (with 0.2 second resolution) and quantifying number zero crossings (corresponding to contractions) in an averaged 10 second window. Photoacoustic spectral response was recorded using a Vevo LAZR (VisualSonics) and placing samples in PE20 tubing submerged in water in the case of nanonaps and concentration-matched gold nanorods with peak absorption at 860 nm. Nanorod concentration was based on gold alone and was provided by the manufacturer (Nanorods LLC). Depth-response in chicken tissue was determined using the home-built photoacoustic system by layering pieces of chicken tissue on top of tubes containing ZnBNc and ONc nanonaps absorption-matched to 400. 2 and 1.5 mJ/cm² pulse energies were recorded at the 710 nm and 860 nm wavelengths used to excite the ZnBNc and ONc nanonaps, respectively. For intestinal obstruction studies, 12-14 g female CD-1 mice (Harlan) were fasted overnight with access to water. The abdomen was then opened with a 1 cm transverse incision near the stomach and the duodenum was ligated with nylon sutures (VWR #89219-096). Sham-treated mice had no duodenum ligation performed, but otherwise it was an identical procedure. The abdomen skin was sutured closed again and within a few hours, mice were then administered a 100 OD₈₆₀ dose of ONc nanonaps by gavage. 1 hour later, the mice were anesthetized and imaged with the Vevo LAZR system.

Nanonap radiolabelling experiments

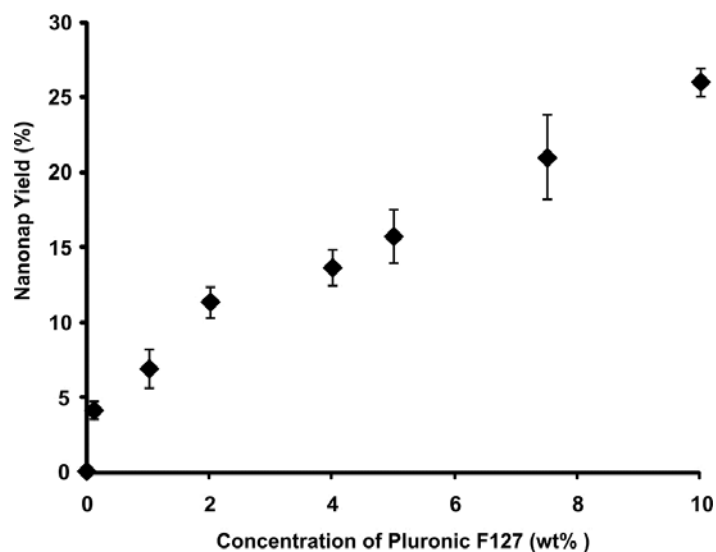
⁶⁴Cu was produced via a ⁶⁴Ni(p,n)⁶⁴Cu reaction using a CTI RDS 112 cyclotron at the University of Wisconsin - Madison. Pilot studies using increasing amount of nanonaps revealed that good radiolabelling yield (> 65%, Supplementary Table 2) could be achieved with as little as 1 µg of nanonaps per 37 MBq of ⁶⁴Cu. Even though PET is more sensitive than PAT for in vivo detection, similar amount of nanonaps was used per mouse to ensure comparable biodistribution patterns between the two studies.

For labelling, 37 MBq of ⁶⁴CuCl₂ was diluted in 300 µL of 0.1 M sodium acetate buffer (pH 5.5) and added into 400 OD nanonaps. The reaction mixture was incubated for 30 minutes at 37 °C with constant shaking. The ⁶⁴Cu-nanonaps were purified by Amicon Ultra-4 centrifugal filter unit (Millipore) with phosphate buffered saline (PBS) as the mobile phase. The final purified ⁶⁴Cu-nanonaps were re-suspended in 500 µL of PBS and used for in vitro stability, oral gavage, PET imaging, and biodistribution studies.

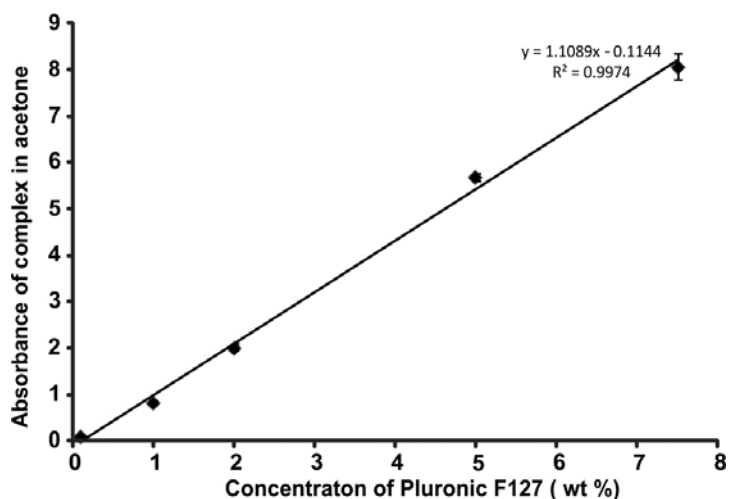
For in vitro chelation stability studies, 37 MBq of ⁶⁴CuCl₂ was incubated with 1 OD of nanonaps for 30 minutes and unconjugated ⁶⁴Cu was separated using 100 kDa cutoff Amicon filters (Millipore, Billerica, MA). After that, one OD of ⁶⁴Cu-nanonaps were re-suspended in 1 mL of SGF or SIF and incubated at 37 °C with stirring. Portions of the mixture (50 µL) were sampled at different time points (0.5, 1, 2, 4, 8, and 24 hours post-incubation) and filtered through 100 kDa cutoff filters. The filtrates were collected and the radioactivity was measured by a Wizard2 automatic gamma counter (Perkin-Elmer, Waltham, MA). The percentages of retained ⁶⁴Cu on the nanonaps were calculated using the following equation: (total radioactivity - radioactivity in filtrate)/total radioactivity. All the experiments were carried out in triplicates.

PET scans were performed using an Inveon microPET/microCT rodent model scanner (Siemens Medical Solutions USA, Inc.). After fasting overnight, each BALB/c mouse was administered with ~7.4 MBq of ⁶⁴Cu-nanonaps (100 ODs in 125 µL PBS) via oral gavage. Five to ten minute static PET scans were performed at various time points post-injection. The images were reconstructed using a maximum a posteriori (MAP) algorithm, with no scatter correction. Region-of-interest analysis of each PET scan was performed using vendor software (Inveon Research Workplace) on decay-corrected whole-body images to calculate the percentage injected dose per gram of tissue (%ID/g) values for intestines.

After the last PET scans at 24 hours post injection, all the mice were euthanized and biodistribution studies were carried out to confirm that the quantitative tracer uptake values based on PET imaging truly represented the radioactivity distribution in mice. Blood and major organs/tissues were collected and wet weighed. The radioactivity in the tissue was measured using a gamma-counter (Perkin Elmer) and presented as %ID/g.



Supplementary Figure 1: Yield of nanonaps as a function of initial F127 concentration. Nanonap yield following nanonap formation in solutions of varying Pluronic F127 concentrations. A 10% (w/v) Pluronic F127 was selected for nanonap formulation since solution viscosity increased beyond this concentration. Mean +/- std. dev. for n=3.



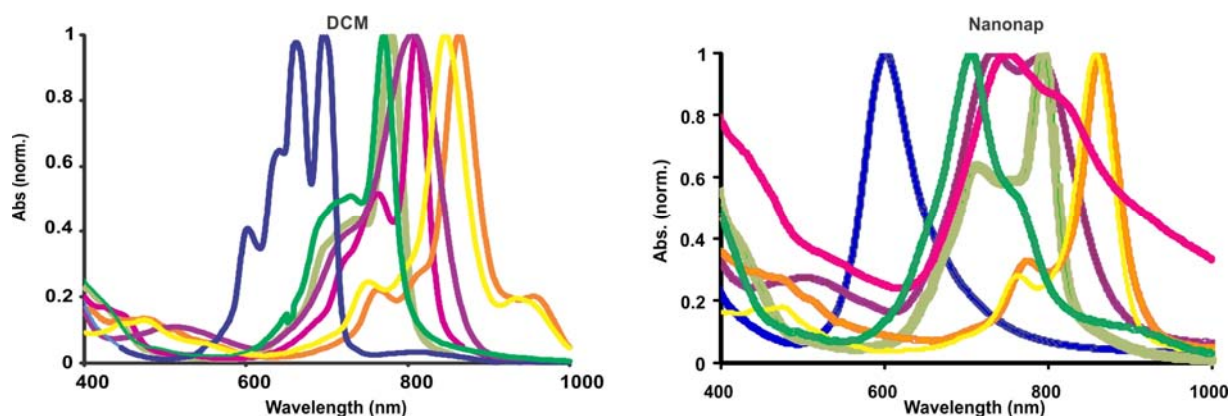
Supplementary Figure 2: Calibration curve used to determine free F127 concentration during centrifugal washing. Pluronic F127 and cobalt thiocyanate formed a dark blue complex (absorbance at 623 nm). The presented data accounts for dilution factors. Mean +/- std. dev. for n=3.



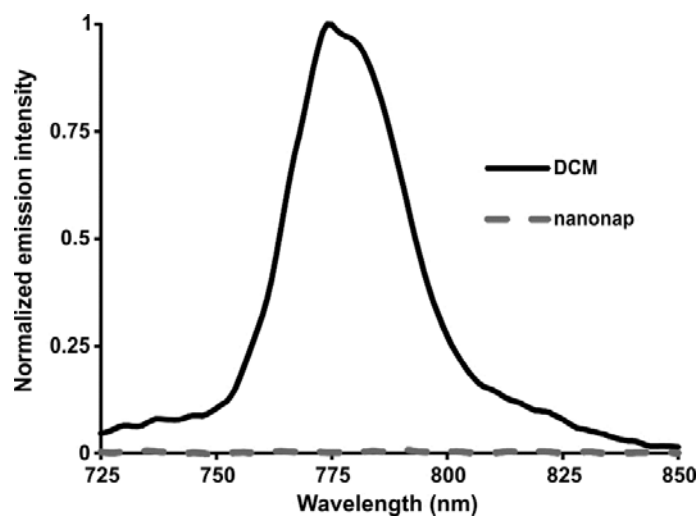
Supplementary Figure 3: Contact angle analysis of washing cycles. Determination of wash numbers required to remove free F127 based on contact angle analysis (angle indicated in figure). Nanonaps were formed in a 10% (w/v) solution of F127 ("Before wash") sample and free F127 was removed following CMC switching using centrifugal wash steps.

Supplementary Table 1: Nanonap optical parameters

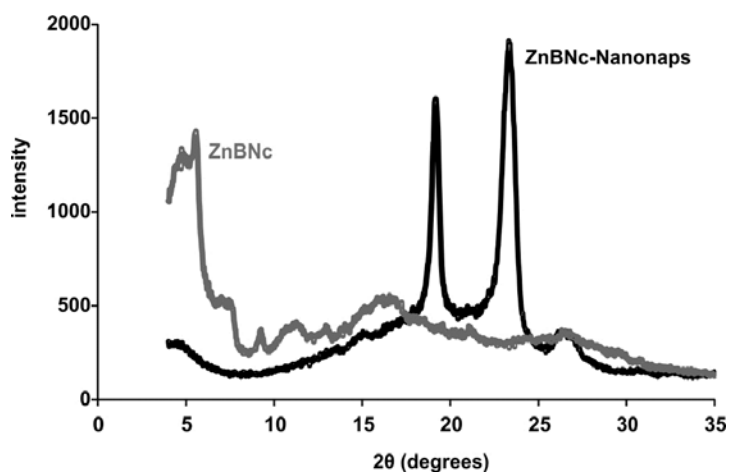
	Pc nanonaps	ZnBNc nanonaps	BNc nanonaps	ONc nanonaps
Peak absorption in dichloromethane	695 nm	780 nm	769 nm	863 nm
Extinction coefficient of dye in dichloromethane	193 ml·mg ⁻¹ ·cm ⁻¹ 1.5×10 ⁵ M ⁻¹ ·cm ⁻¹	100 ml·mg ⁻¹ ·cm ⁻¹ 1.0×10 ⁵ M ⁻¹ ·cm ⁻¹	138 ml·mg ⁻¹ ·cm ⁻¹ 1.3×10 ⁵ M ⁻¹ ·cm ⁻¹	172 ml·mg ⁻¹ ·cm ⁻¹ 2.2×10 ⁵ M ⁻¹ ·cm ⁻¹
Peak absorption in aqueous nanonap form	600 nm	707 nm	793 nm	860 nm
Extinction coefficient of dye within aqueous nanonaps	52 ml·mg ⁻¹ ·cm ⁻¹ 3.8×10 ⁴ M ⁻¹ ·cm ⁻¹	33 ml·mg ⁻¹ ·cm ⁻¹ 3.3×10 ⁴ M ⁻¹ ·cm ⁻¹	59 ml·mg ⁻¹ ·cm ⁻¹ 5.5×10 ⁴ M ⁻¹ ·cm ⁻¹	118 ml·mg ⁻¹ ·cm ⁻¹ 1.5×10 ⁵ M ⁻¹ ·cm ⁻¹
Molar ratio of dye to F127 in nanonap	5.4	3.9	0.2	3.2
Molecular weight of nanonaps	1.6×10 ⁶ g·mol ⁻¹	2.6×10 ⁶ g·mol ⁻¹	5.7×10 ⁶ g·mol ⁻¹	2.6×10 ⁶ g·mol ⁻¹
Number of ONCs per nanonap	526	621	106	501
Number of F127 per nanonap	98	158	488	155
Nanonap extinction coefficient	12.5 ml·mg ⁻¹ ·cm ⁻¹ 2.0×10 ⁷ M ⁻¹ ·cm ⁻¹	7.6 ml·mg ⁻¹ ·cm ⁻¹ 2.0×10 ⁷ M ⁻¹ ·cm ⁻¹	1.0 ml·mg ⁻¹ ·cm ⁻¹ 5.8×10 ⁷ M ⁻¹ ·cm ⁻¹	29.2 ml·mg ⁻¹ ·cm ⁻¹ 7.6×10 ⁷ M ⁻¹ ·cm ⁻¹
Nanonap optical absorption cross section	7.7×10 ⁻¹⁸ m ²	7.6×10 ⁻¹⁸ m ²	2.2×10 ⁻¹⁸ m ²	2.9×10 ⁻¹⁷ m ²



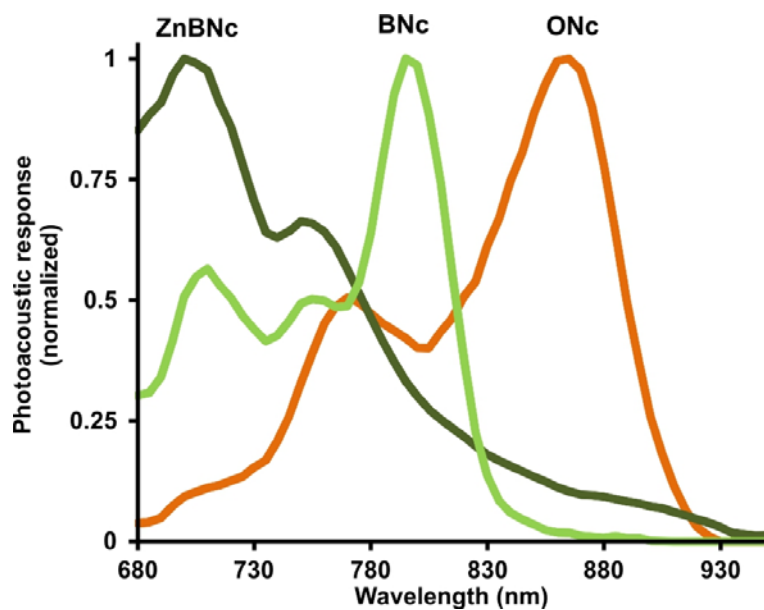
Supplementary Figure 4: Normalized absorbance spectrum of Nc dyes in dichloromethane and in aqueous nanonap forms. BPC, ZnBNc, BNc, VBPC, VBNC, ONc, NiONc are shown in blue, dark green, yellow green, purple, pink, amber and yellow, respectively. Shifted absorbance spectra of successfully formed nanonaps compared to the dichloromethane spectra indicated the dense arrangement of Nc dyes in nanonaps modified some electronic properties.



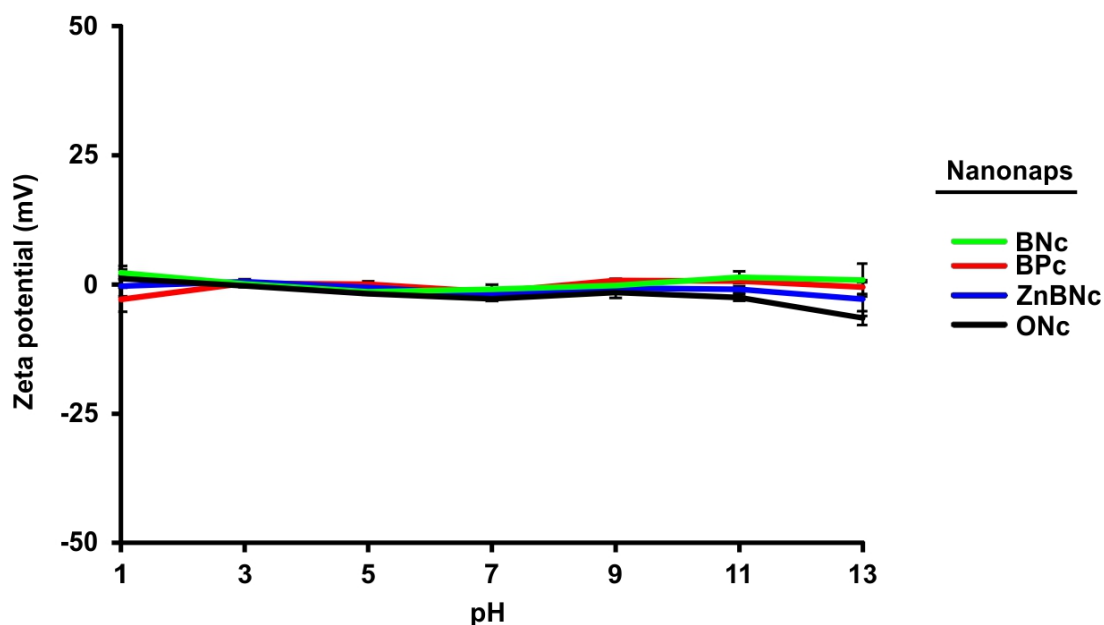
Supplementary Figure 5: Self-quenched fluorescence emission of ZnBNC nanonaps. Fluorescence of absorption-matched ZnBNC nanonaps in water and free ZnBNC in dichloromethane (DCM).



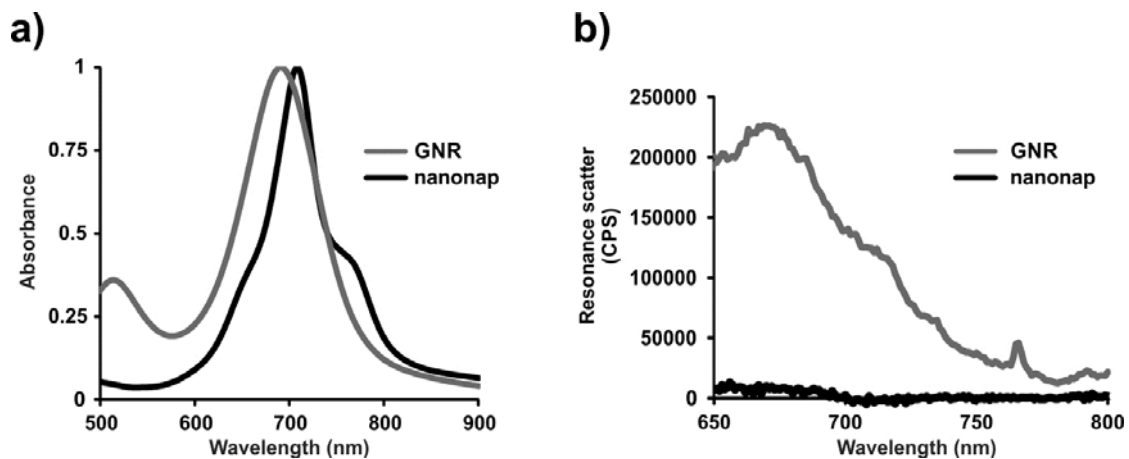
Supplementary Figure 6: X-ray diffraction spectrum of freeze-dried ZnBNC nanonaps and pure ZnBNC. Although ZnBNC (grey line) exhibits weak crystallization properties compared to Pluronic F127, small peaks indicate some crystallization orientation (at 7°). However, these disappeared after nanonap formation (black line). The two large peaks observed in nanonaps are due to characteristic Pluronic F127 crystal patterns based on PEO crystallinity.



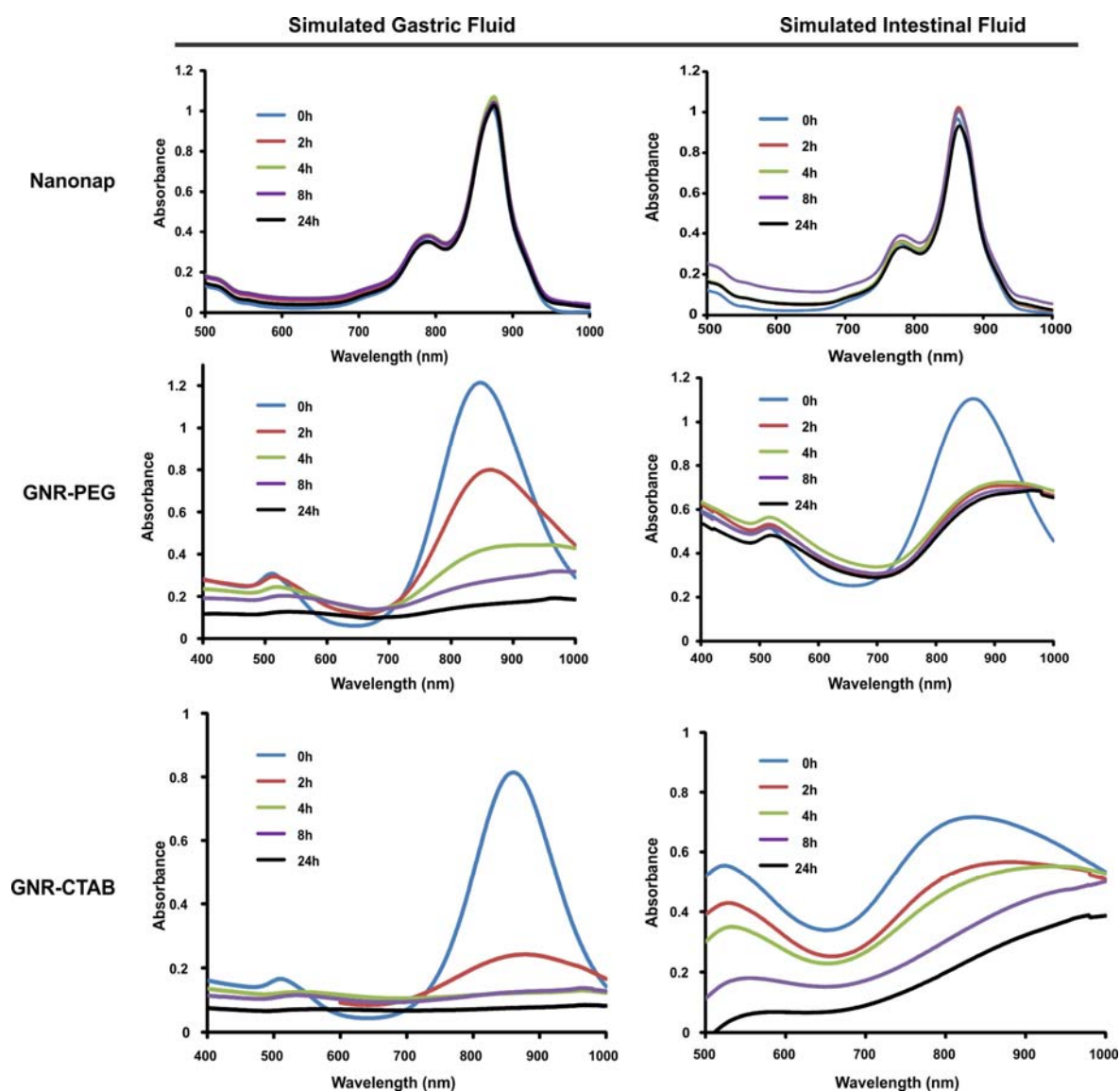
Supplementary Figure 7: Photoacoustic spectra of ZnBnC, BNc and ONc nanonaps. The maximal absorbance of the indicated nanonaps was adjusted to 10 and PA spectral scans were conducted in PE20 tubing on a Vevo LAZR.



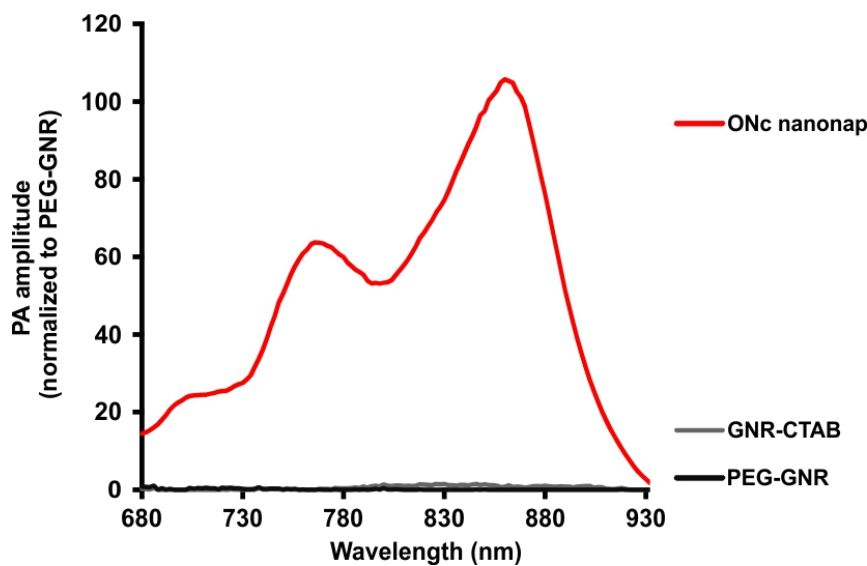
Supplementary Figure 8: Nanonaps maintain near neutral zeta potential over broad pH range. Nanonaps were diluted into pH-adjusted phosphate buffer and zeta potential was recorded. Mean +/- std. dev. for n=3



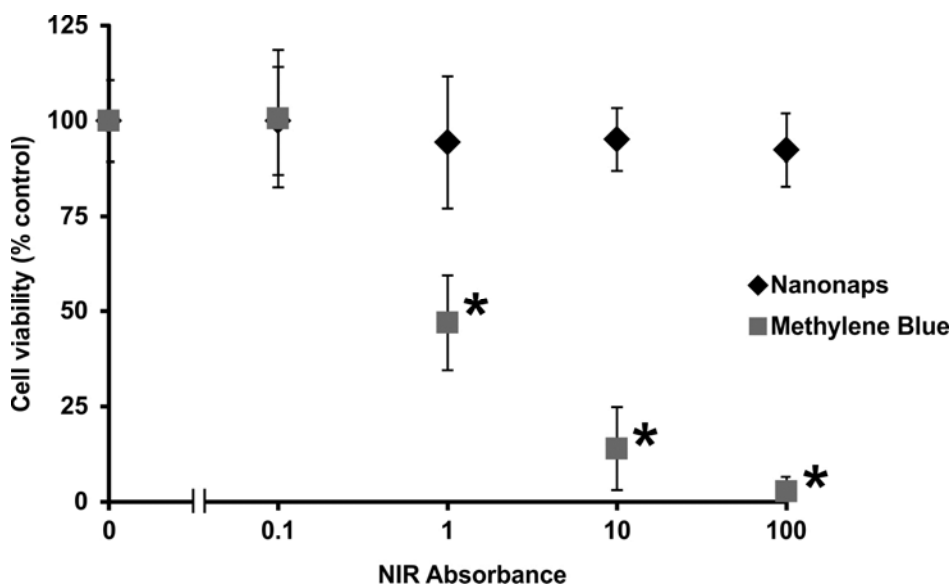
Supplementary Figure 9: Resonance scattering spectra of nanonaps and gold nanorods. a) ZnBnC nanonaps and gold nanorods (GNR) concentration was adjusted to normalize the absorbance at wavelength of 700 nm. 50 μ L were diluted in 950 μ L water for resonance light scattering analysis. The final extinction of nanonaps and GNR was equal 0.05 at 700 nm. b) Resonance light scattering was carried out using nanonaps and GNR (absorbance=0.05) on a spectrofluorometer with the excitation and emission slit width adjusted to 2 nm. Buffer scattering blanks were subtracted. Representative of 3 independent trials.



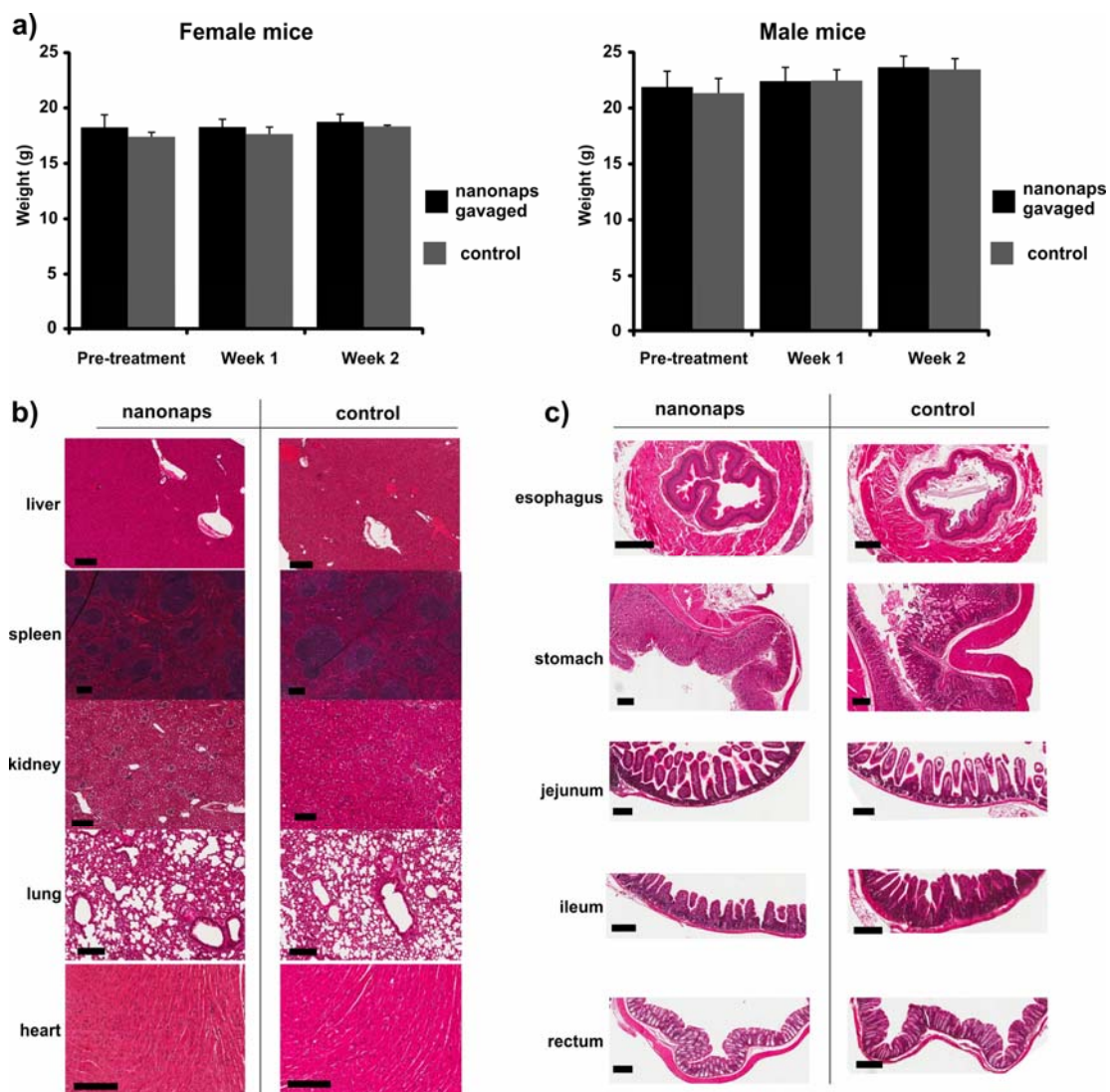
Supplementary Figure 10: Nanonaps, but not gold nanorods, are stable in simulated gastric and intestinal fluid. Nanonaps and gold nanorods stabilized by thiol-PEG or residual CTAB were diluted into simulated gastric fluid (SGF) or simulated intestinal fluid (SIF) and dialyzed at 37 °C in those solutions. Solution absorbance was measured at the indicated time points. Data shown is representative of 3 independent trials for all time points and conditions.



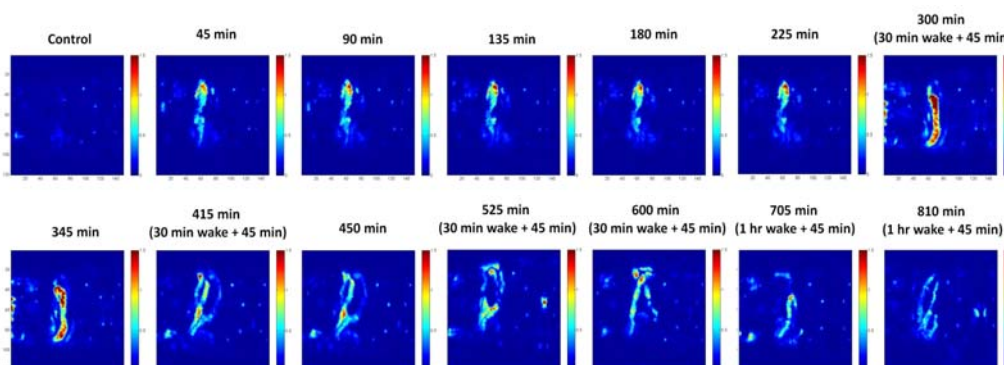
Supplementary Figure 11: Photoacoustic spectra of concentration-matched nanonaps and gold nanorods. ONc nanonaps and gold were normalized to 1.2 mg/mL concentration and photoacoustic spectra was recorded on a Vevo LAZR. Nanorod mass is based on gold alone. Representative of three separate trials.



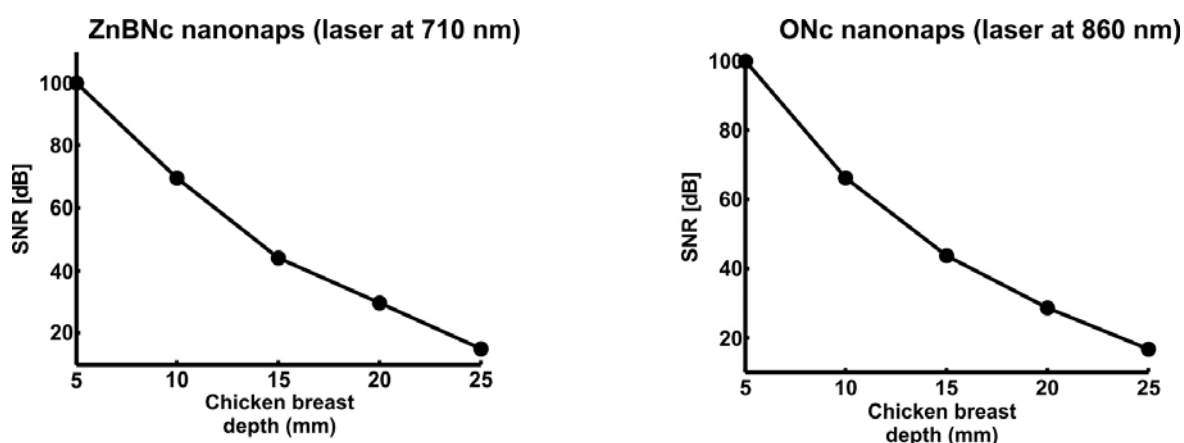
Supplementary Figure 12: Caco-2 cell viability following incubation with nanonaps or methylene blue. Concentrated ONc nanonaps and methylene blue solutions were diluted into Caco-2 cell medium, with final NIR absorbances as indication. Cells were incubated with dyes for 24 hours in DMEM media with 20% serum at 37 °C, then viability was assessed using the XTT assay. Mean \pm std. dev. for n=6. No statistically significant difference was found between control and any of the nanonap-treated groups, based on one-way ANOVA. For methylene blue, the asterisks mark statistically significant groups from the untreated control based following one-way ANOVA and Tukey's posthoc analysis ($p < 0.001$).



Supplementary Figure 13: 50,000 OD₈₆₀/kg nanonaps is a safe orally-administered nanonap dose. a) Mouse mass following gavage of 1000 OD doses. Within the 2-week period, mice displayed no signs of distress or abnormal behaviour. Mean \pm std. dev for n=5 mice for each male (\pm nanonap) and female (\pm nanonap) group. No statistically significant differences were observed between the mass of treated and control mice following study completion (based on 2-tailed students t-test, $P > 0.05$) **b)** Histology of H&E stained liver, spleen, kidneys, lungs and heart from treated or control mice. No signs of systemic toxicity were observed. **c)** Histology of organs of the GI tract including the oesophagus, stomach, small intestine and large intestine revealed no obvious damage based on H&E staining. All scale bars represent 200 μ m.



Supplementary Figure 14: Lack of motility of nanonaps in mice anesthetized with 3% v/v isoflurane. Mice were administered 3% v/v isoflurane in pure oxygen continuously while PAT scans were conducted except 6 time intervals (225-255 min, 345-375 min, 450-480 min, 525-555 min, 600-660 min, 705-765 min) when isoflurane was removed to let the mouse wake up. No significant movement was observed during heavy anesthetization and motility was restored after the removal of isoflurane.

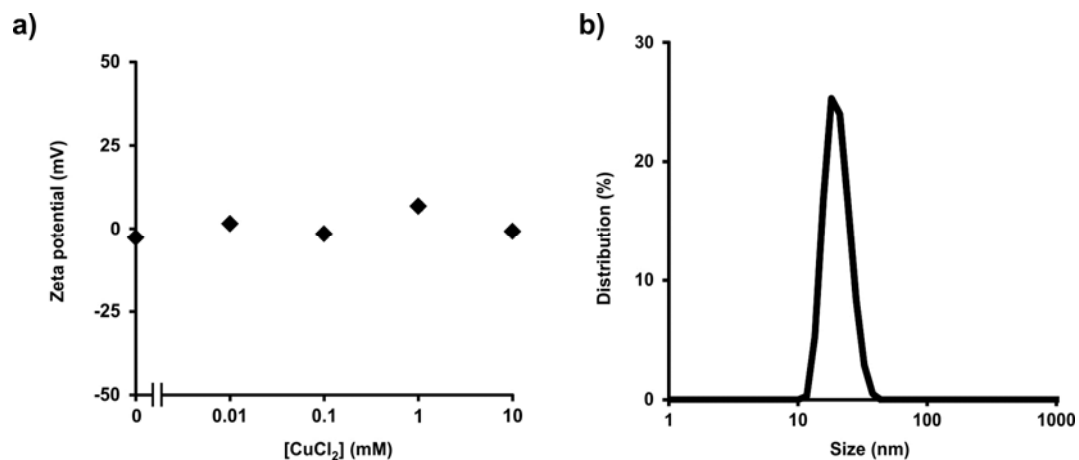


Supplementary Figure 15: Signal to noise ratio of ZnBNC and ONc nanonaps in a chicken breast phantom. Absorbance matched (absorbance of ~400) ZnBNC and ONc nanonaps were placed in a chicken phantom and photoacoustic signal was monitored with progressive addition of chicken breast tissue. Energy pulse densities were 2 and 1.5 mJ/cm² at 710 nm and 860 nm respectively.

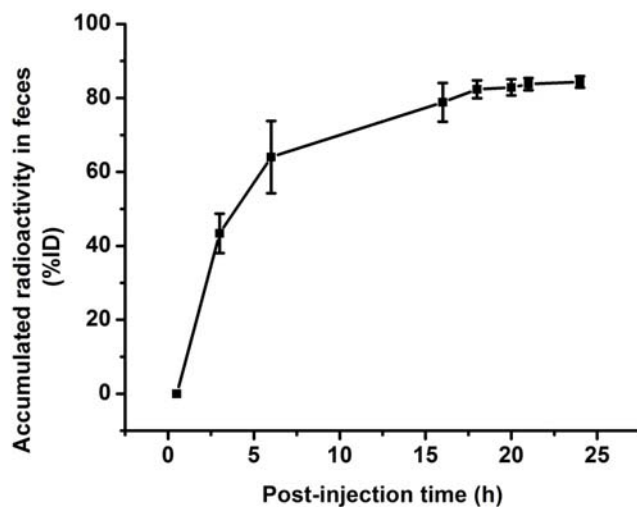
Supplementary Table 2: Labelling of nanonaps with ⁶⁴Cu

Radiolabelling yield using different amount of nanonaps per mCi of ⁶⁴Cu. Data represent mean ± SD. for triplicate experiments except at the largest dose which was a single experiment.

0.25 µg/mCi	41.1 +/- 3.8%
1 µg/mCi	65.1 +/- 2.6%
5 µg/mCi	74.9 +/- 1.1 %
25 µg/mCi	73.0% +/- 1.9%
100 µg/mCi	80.5%



Supplementary Figure 16: Copper labelling does not affect nanonap zeta potential or size. ONc nanonaps (100 ODs) were incubated in 0, 0,01, 0.1, 1, 10 mM cold CuCl₂ at 37 °C for 30 minutes with constant shaking. Labelled nanonaps were washed 4 times with centrifugal filtration to remove excess copper and zeta potential was measured. Mean+/- std. dev. for n=3. Size is shown for 10 mM labelling conditions.



Supplementary Figure 17: Faecal clearance of ⁶⁴Cu chelated in nanonaps. Following radiolabelling, mice were given 100 ODs of nanonaps by gavage (7.4 MBq per mouse). Faeces were collected and analysed with gamma counting.